A Truly-Explicit Adaptive Time-Integration Approach for Elastodynamic Analyses

Lucas Ruffo Pinto[1], Delfim Soares Jr.[2], Webe João Mansur[1], Cristhian A. C. Cortez[3], Ricardo S. N. Bragança[3], Eduardo G. D. Carmo[1]
COPPE / Federal University of Rio de Janeiro, [2]Structural Engineering Department / Federal University of Juiz de Fora,[3]Petrobras

This paper was prepared for presentation during the 18th International Congress of the Brazilian Geophysical Society held in Rio de Janeiro, Brazil, 16-19 October 2023.

Abstract

In this paper, a new explicit time-marching procedure for solving elastodynamic problems in the time domain is discussed. The procedure is designed to adapt to the properties of the spatially discretized model and is completely automated, making it highly effective for analyzing complex wave propagation models. The approach is accurate to second order, fully explicit, and truly self-starting, with the added benefits of adaptive algorithmic dissipation and extended stability limits. To further improve performance, the procedure also includes automated subdomain/sub-cycling splitting procedures. By automatically dividing the model domain into multiple subdomains based on the properties of the discretized problem, the procedure applies different time-step values while still ensuring stability and enabling more accurate and efficient analyses. Additionally, the procedure considers adaptive values for the time-integration parameters, which are determined based on the spatial discretization, to create a locally-defined self-adjustable formulation. This approach establishes a link between the applied spatial and temporal solution procedures, better counterbalancing their errors. The paper presents and discusses expressions for the adaptive time-integration parameters and limiting time-step values of the discretized domain elements. Finally, benchmark analyses are conducted to demonstrate the technique's effectiveness, taking into account theoretical problems and complex models, representative of real-world applications in the OIL & GAS industry.

Introduction

Wave propagation models require spatial and temporal discretization techniques for numerical solution. In practice, spatial discretization methods are initially considered to generate a semi-discrete time-domain system of equations. Finite element formulations based on local approximations have been successfully used in engineering to solve partial differential equation problems. However, local approximations are mostly based on temporal and/or spatial definition of the time-step value when solving equations that require time integration. Numerical methods are commonly used to solve time-dependent hyperbolic equations, as their analytical resolution is often unfeasible. These methods use step-by-step time integration algorithms with temporal discretization, which are divided into two groups: explicit methods (computationally effective but with stability restrictions) and implicit methods (may provide unconditional stability but are more computationally expensive per time step).

A new approach for locally defined time-marching formulations is discussed, which combines an adaptive truly explicit time-integration procedure with adaptive time-steps/sub-cycling splitting procedures, creating an effective time-domain solution approach [1]. The time-steps and time-integration parameters are adaptively computed based on the adopted spatial discretization and model properties, making the formulation entirely automated and user-friendly. This novel method is second-order accurate, truly self-starting, and allows for extended stability limits and controllable algorithm dissipation. Algorithm dissipation is crucial to eliminate high frequency spurious numerical contributions in computed responses, and this approach offers a way to efficiently eliminate these spurious frequencies. While many implicit time-marching procedures with dissipative properties are available, algorithm dissipation is also important for explicit time-marching algorithms, as shown by previous studies [1-10].

In the present approach, the time-integration parameters are formulated to dissipate spurious high-modes, while maintaining the contribution of important low-frequency modes, resulting in an accurate dissipative time-marching technique. The effectiveness of the solution procedure can be further improved by using proper multiple time-step values along the model, as in the case of sub-cycling splitting techniques. Truly explicit approaches can disregard solver procedures, but the stability limit becomes a function of the material damping, requiring lower time-step values for physically damped models. However, this work presents an efficient solution methodology for these challenging configurations, allowing relatively high time-step values to be considered in these analyses.

The methodology presented in this study has potential for solving problems in various fields; however, it is primarily focused on elastodynamic analyses and geophysical applications. In geophysics, it is common to encounter heterogeneous domains with multiple layers of various materials that need to be analyzed. Automatic sub-cycling techniques are particularly useful in this regard because they allow for efficient analysis of these different layers or media by dividing them into appropriate subdomains.

Governing equations and time integration strategy

The set of equations that govern a semi-discrete dynamic model can be expressed as:

$$\mathbf{M}\ddot{\mathbf{U}}(t) + \mathbf{C}\dot{\mathbf{U}}(t) + \mathbf{K}\mathbf{U}(t) = \mathbf{F}(t) \qquad (1)$$

where $\mathbf{M}$, $\mathbf{C}$, and $\mathbf{K}$ stand for the mass, damping, and stiffness matrix, respectively. The acceleration, velocity, and displacement of the system are represented by vectors $\ddot{\mathbf{U}}(t)$, $\dot{\mathbf{U}}(t)$ and $\mathbf{U}(t)$, respectively, while the external force acting on the system is represented by the vector $\mathbf{F}(t)$. The initial conditions are defined as $\mathbf{U}^0 = \mathbf{U}(0)$ and $\dot{\mathbf{U}}^0 = \dot{\mathbf{U}}(0)$, representing the initial displacement and velocity vectors, respectively. As this manuscript focuses on explicit analyses, lumped mass matrices are used to define the discretized model described above, as usual. This approach avoids the need to solve systems of algebraic equations when using truly-explicit time-marching formulations, leading to significantly more efficient analyses. Additionally, classical Rayleigh damping is considered in this paper, where the viscous damping matrix $\mathbf{C}$ is assumed to be proportional to the mass and stiffness matrices of the model (i.e., $\mathbf{C} = \alpha_m\mathbf{M} + \alpha_k\mathbf{K}$, where α_m and α_k are constants of proportionality).

The time integration procedure discussed here is an extension of the first methodology presented by Soares [11], which proposed three truly-explicit time-marching procedures for the semi-discrete system of equations (1) using proper coefficients and chained compositions of stiffness and damping matrix multiplications to develop efficient second-, third-, and fourth-order accurate time-domain solution procedures. As a result, the present time-integration procedure may be defined by the following recurrence relationships:

$$\mathbf{M}\mathbf{V}_1 = \int_{t^n}^{t^{n+1}} \mathbf{F}(t)\,dt - \Delta t[\mathbf{C}\dot{\mathbf{U}}^n + \mathbf{K}(\mathbf{U}^n + \frac{1}{2}\Delta t\dot{\mathbf{U}}^n)] \quad (2a)$$

$$\mathbf{M}\mathbf{V}_2 = \Delta t\mathbf{C}\mathbf{V}_1 \quad (2b)$$

$$\dot{\mathbf{U}}^{n+1} = \dot{\mathbf{U}}^n + \mathbf{V}_1 - \frac{1}{2}\mathbf{V}_2 \quad (2c)$$

$$\mathbf{M}\mathbf{V}_3 = \Delta t\mathbf{K}(\mu_1\Delta t\dot{\mathbf{U}}^{n+1} + \mu_2\Delta t\dot{\mathbf{U}}^n) \quad (2d)$$

$$\mathbf{U}^{n+1} = \mathbf{U}^n + \frac{1}{2}\Delta t(\dot{\mathbf{U}}^n + \dot{\mathbf{U}}^{n+1} - \mathbf{V}_3) \quad (2e)$$

where Δt represents the time-step of the analysis, and auxiliary vectors $\mathbf{V}_1$, $\mathbf{V}_2$ and $\mathbf{V}_3$ are defined as indicated by equations (2a), (2b) and (2d). The auxiliary vector $\mathbf{V}_3$ is evaluated at an element level, taking into account the local features of the spatially discretized model, which are accounted for when locally computing the time-integration parameters μ_1 and μ_2. In this case, at the element level, a local vector $\mathbf{V}_e$ is computed as $\mathbf{V}_e = \mathbf{K}_e(\overline{\mu}_1^e\dot{\mathbf{U}}_e^{n+1} + \overline{\mu}_2^e\dot{\mathbf{U}}_e^n)$, where the subscripts and superscripts "e" indicate that the related variables are defined at an element level (and $\overline{\mu}_i^e = \Delta t\,\mu_i^e$), and a vector $\mathbf{V}$ is assembled by composing $\mathbf{V}_e$. $\mathbf{V}_3$ is finally computed as $\mathbf{V}_3 = \Delta t\mathbf{M}^{-1}\mathbf{V}$, following equation (2d). This locally defined approach enables the specification of μ_1 and μ_2 for each element of the discretized model, considering local properties, resulting in a more effective solution procedure.

In this work, the following expressions are considered to define μ_1^e and μ_2^e:

$$\mu_1^e = 4(\xi_e\Omega_e^{max} - 1)^{-1}\Omega_e^{max-4} + 4\xi_e\Omega_e^{max-3} + 2\Omega_e^{max-2} \quad (3a)$$

$$\mu_2^e = -2(\xi_e\Omega_e^{max} - 1)^{-1}\Omega_e^{max-4} - 4\xi_e\Omega_e^{max-3} \quad (3b)$$

where $\Omega_e^{max} = \omega_e^{max}\Delta t$ and $\xi_e = \alpha_m(2\omega_e^{max})^{-1} + \frac{1}{2}\alpha_k\omega_e^{max}$ are defined as the maximal sampling frequency and damping ratio of element "e", respectively, where ω_e^{max} stands for the highest natural frequency of the element. Expressions (3a-b) are formulated to nullify the spectral radius of the method at Ω_e^{max}, providing maximal numerical damping at the highest sampling frequency of the element. This design optimizes the formulation to reduce the influence of spurious high-frequency modes, allowing for enhanced analyses. The goal of introducing numerical damping is to eliminate non-physical spurious oscillations caused by unresolved modes. However, designing a dissipative algorithm that introduces high-frequency dissipation without affecting low-frequency modes is challenging. The new methodology adapts by enforcing low spectral radius values at the highest frequencies and relatively high spectral radius values at important low frequencies.

As it is commonly known, when non-zero values of α_k are used, physical damping is already incorporated at the highest frequencies of the model. Therefore, there is no need to introduce numerical damping into the analysis, and the values of $\mu_1^e = \mu_2^e = 0$ can then be adopted, which eliminates the need to evaluate equation (2d) and further enhances the efficiency of the solution algorithm. Thus, in this study, if $\xi_e \geq 0.222$ (see [1] for further details about this value), numerical damping is not applied in the analysis, and time integration parameters are set to zero (i.e., $\mu_1^e = \mu_2^e = 0$).

The solution algorithm described by equations (2a-e) is easy to implement and requires no input information from the user as all parameters are automatically evaluated based on the model's properties. The technique is self-starting and truly explicit, requiring no treatment of any system of equations and only the "inversion" of the diagonally adopted $\mathbf{M}$ matrix. The proposed time-marching formulation establishes a link between the spatial and temporal discretization procedures, allowing for better error balance and more accurate responses. The technique provides enhanced accuracy and improved stability conditions, with a stability limit more than 1.7 times greater than that of the Central Difference method (CDM). The limiting time-step value for each element of the discretized model can be established considering two possible configurations, depending on whether $\mu_1^e = \mu_2^e = 0$ or not, as indicated below:

$$\text{if } \xi_e \leq 0.222, \qquad \Delta t_e = (2 + 2^{1/2})(\omega_e^{max})^{-1} \quad (4a)$$

$$\text{if } \xi_e > 0.222, \qquad \Delta t_e = (\xi_e\omega_e^{max})^{-1} \quad (4b)$$

As can be seen from equations (4a-b), the proposed technique allows for easy estimation of the limiting time-step value, which is not common in standard truly explicit approaches. This estimation is important for the automated subdomain divisions and adaptive computations of local

time-step values discussed in the next subsection. Finally, a minimal value of Ω_e^{max} in equations (3a-b) is suggested to avoid excessive numerical damping when subdomain/sub-cycling splitting procedures are not considered, with a value of $2^{1/2}$ recommended.

Sub-cycling

Sub-cycling is a technique proposed by Belytschko et al. [12] that decomposes a domain into subdomains associated with computations at several "sub-steps". This approach enables an explicit time-marching solution without limiting the entire domain to its shortest critical time-step value, allowing greater time-step values to be considered for different subdomains and enabling lower computational efforts. The need for using sub-cycling arises from problems where meshes include both relatively stiff and soft subdomains, imposing the use of an overly small time-step value for the entire model. Therefore, to enable an efficient computational approach, one must solve these regions separately, considering different time-step values for different subdomains of the model, and connect the computed responses from these subdomains together. However, excessive subdivisions may result in deterioration in both accuracy and efficiency, highlighting the importance of proper sub-cycling considerations.

This study proposes an automated algorithm to subdivide the model domain, aiming to enhance efficiency without compromising accuracy [13]. The algorithm performs a controlled subdivision of the domain, computing and assigning a time-step (Δt) for each node of the model. The procedure consists of grouping elements that can share the same Δt, based on their stability limit. By doing so, the model is divided into subdomains, and different time-step values are assigned to each subdomain, allowing for an efficient and accurate solution. In this context, the following sequence of commands is here employed to automatically define this subdomain division: (i) calculate the limiting time-steps of all elements (i.e., Δt_e) following equations (4a-b), finding the smallest Δt_e of the model (i.e., Δt_e^{min}, where $\Delta t_e^{min} = \min(\Delta t_e)$), which is the basic time-step for the proposed controlled subdivision of the domain; (ii) with Δt_e^{min} defined, calculate subsequent time-step values as multiple of the power of 2 of this minimal time-step value (i.e., calculate Δt_i, where $\Delta t_i = 2^{(i-1)}\Delta t_e^{min}$); (iii) associate each element to a computed time-step value (i.e., to Δt_i, where $\Delta t_i \leq \Delta t_e \leq \Delta t_{i+1}$ and i indicates the subdomain of that element); (iv) associate a time-step value (i.e., associate a subdomain) to each degree of freedom of the model considering the lowest time-step value of its surrounding elements.

After implementing the subdomain division and sub-cycling algorithm, it may be necessary to interpolate the displacement and velocity values near the boundaries of the time-step subdomains. This work employs the following expressions for these interpolations:

$$\mathbf{U}(t) = \frac{1}{2\Delta t}\left(\dot{\mathbf{U}}^{n+1} - \dot{\mathbf{U}}^{n}\right)t^2 + \dot{\mathbf{U}}^{n}t + \mathbf{U}^{n} \quad (5a)$$

$$\dot{\mathbf{U}}(t) = \frac{1}{\Delta t}\left(\dot{\mathbf{U}}^{n+1} - \dot{\mathbf{U}}^{n}\right)t + \dot{\mathbf{U}}^{n} \quad (5b)$$

where t is the current increment of time ($0 \leq t \leq \Delta t$) for the focused subdomain and Δt is the time-step value of the degree of freedom being interpolated, which is related to the neighboring subdomain. A similar expression to equation (5b) is used to interpolate $\mathbf{V}_1$, if required, based on equation (2b).

Numerical applications

This study examines the performance of the proposed solution procedure using two elastodynamic models. The first model is a heterogeneous rod composed of two materials, for which analytical solutions are available, allowing to evaluate the accuracy of the proposed technique. The second model is a synthetic model with degrees of complexity similar to real geological applications, demonstrating the efficacy of the proposed methodology for analyzing large geophysical problems, such as those encountered in the OIL & GAS industry. Specifically, this study considers the elastic 2DEW model, which features multiple layers with varying properties and large salt regions, representing complex configurations of elastodynamic wave propagation.

The results obtained from the proposed novel adaptive formulation, with (New/sub) or without (New) considering multi-time-steps/sub-cycling splitting procedures, were compared to those of standard explicit approaches. These approaches included the classic Central Difference (CD) method, the explicit generalized α (EG-α) method developed by Hulbert and Chung [14] (where ρb = 0.3665 was adopted, as this value is recommended by the authors to minimize period elongation errors), and the Noh-Bathe (NB) method [2] (where p = 0.54 was adopted, as recommended by the authors). For each technique, the maximum possible time-step value for stability was applied (taking into account an element level evaluation) to allow for more efficient analyses to be conducted for each approach.

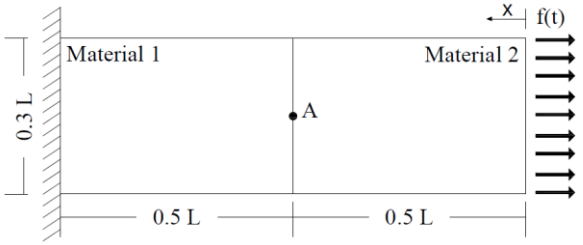

Fig.1 – Sketch of the heterogeneous rod.

Application 1

In this study, a rectangular heterogeneous rod consisting of two different materials is analyzed. A schematic of the rod is presented in Figure 1, and the physical properties of the materials used to compose each half of this heterogeneous model are described in Table 1. Five different heterogeneous configurations are considered in this section, and in all of them, material 1 is assumed to be lead, while material 2 can be lead (model 1 - homogeneous model), copper (model 2), steel (model 3), alumina (model 4), or carbon nanotubes (model 5). A structured finite element mesh composed of 20,000 linear square elements is utilized to spatially discretize the model. The analytical

solution for the horizontal displacements of the rod is known in the literature and can be found in [1], allowing for proper evaluation of the accuracy of the proposed solution technique.

Table 1 – Properties of the materials for the second example

Material	Young's modulus (MPa)	Density (Kg/m^3)	Dilatational wave speed (m/s)
Lead	14	11340	1111
Copper alloys	135	8300	4033
Steel	200	7860	5044
Alumina	390	3900	10000
Carbon nanotube	1000	1700	24253

Table 2 presents the performances of the selected time-integration techniques for both the adopted heterogeneous model and the homogeneous model 1. The new methodology provides the smallest errors and CPU times for the performed analyses, and better results are obtained when multi-time-steps/sub-cycling splitting approaches are considered, indicating that the proposed formulation is highly accurate and efficient. Additionally, the new technique becomes more effective when it can adapt to the properties of the model, as in the referred heterogeneous models. For the selected heterogeneous models, two time-marching subdomains are always established, and the time-steps of neighboring subdomains differ up to 16 times in this example. Nevertheless, good responses are always provided, illustrating the robustness of the proposed technique.

Table 2 – Performance of the methods for application 1

Model	Method	Δt (10^{-6}s)	Error (10^{-2})	CPU Time (s)
1	CD	7.199 (1.10)	0.18 (1.80)	17 (1.21)
	EG-α	6.487 (1.00)	0.16 (1.59)	19 (1.35)
	NB	13.480 (2.07)	0.17 (1.65)	21 (1.50)
	New	12.912 (1.99)	0.10 (1.00)	14 (1.00)
2	CD	1.884 (1.10)	6.31 (5.00)	23 (1.43)
	EG-α	1.698 (1.00)	6.24 (4.95)	24 (1.50)
	NB	3.528 (2.07)	6.14 (4.87)	26 (1.62)
	New	3.386 (1.99)	2.23 (1.77)	20 (1.25)
	New/sub	6.770[b] (3.98)	1.26 (1.00)	16 (1.00)
3	CD	1.506 (1.10)	11.17 (2.97)	29 (1.93)
	EG-α	1.357 (1.00)	10.72 (2.85)	31 (2.06)
	NB	2.821 (2.07)	10.66 (2.83)	32 (2.13)
	New	2.707 (1.99)	4.60 (1.23)	25 (1.67)
	New/sub	1.082[b] (7.97)	3.76 (1.00)	15 (1.00)
4	CD	0.759 (1.10)	16.96 (4.79)	44 (2.31)
	EG-α	0.684 (1.00)	17.00 (4.80)	52 (2.73)
	NB	1.432 (2.07)	16.67 (4.71)	54 (2.84)
	New	1.365 (1.99)	5.57 (1.57)	37 (1.94)
	New/sub	10.920[b] (15.96)	3.53 (1.00)	19 (1.00)
5	CD	0.313 (1.10)	25.80 (4.90)	77 (2.85)
	EG-α	0.282 (1.00)	25.82 (4.90)	92 (3.40)
	NB	0.586 (2.07)	25.98 (4.93)	96 (3.55)
	New	0.563 (1.99)	8.56 (1.62)	69 (2.55)
	New/sub	9.008[b] (31.94)	5.26 (1.00)	27 (1.00)

Relative values are provided in parenthesis; [b] Maximal Δt in the multiple time-steps analysis.

Application 2

The second example considers a geophysical model generated in SEAM, simulating a realistic soil of a salt region in the Gulf of Mexico, complete with stratigraphy in a scale that includes oil and gas reservoirs. All model properties are derived from fundamental rock properties, which have subtle contrasts at the boundaries of the macro-layer, generating realistic synthetic data. The distribution used, Elastic Earth Model, is the model used for simulating the elastic data set, Elastic 2DEW Classic [15]. The distribution used has 3 binary files for density, P-wave velocity (dilation), and S-wave velocity (shear).

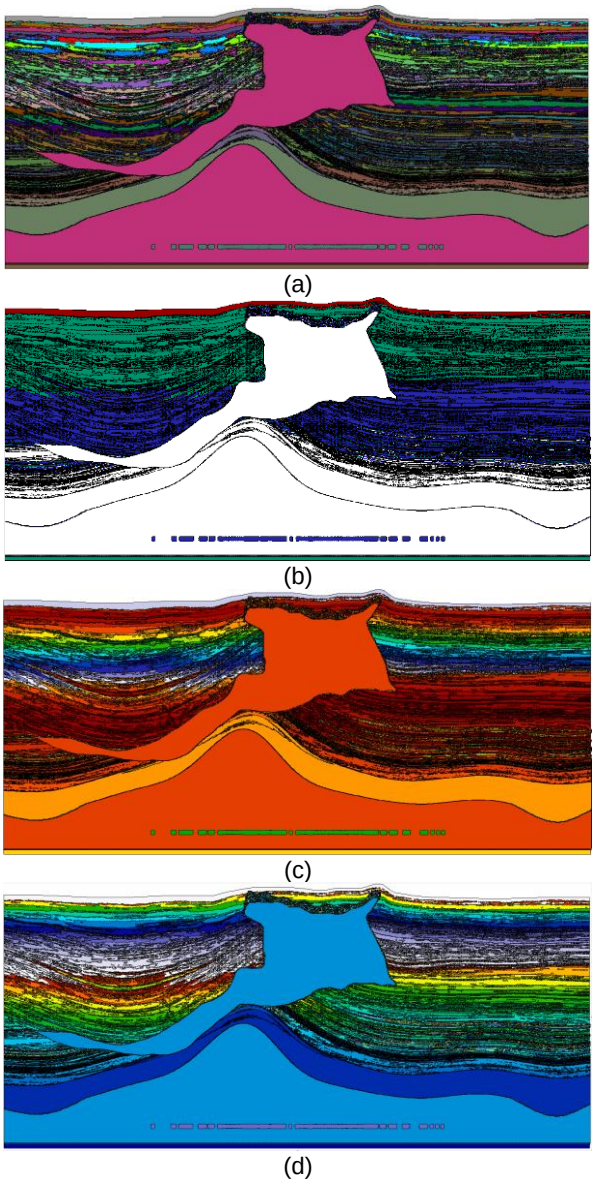

Fig.2 – Geological model: (a) layers illustrating its different physical properties; (b) layers illustrating the computed different time-marching subdomains; computed time-integration parameters (c) μ_1^e and (d) μ_2^e.

The model depicted in Figure 2a has an area of 35 km x 15 km and is discretized by a mesh of 717,139 linear triangular elements. A pulse is applied to its surface at x = 17.44 km. In the model, the salt regions are described using finer discretizations than the earth layers. Four Δt subdomains were automatically established, as shown in Figure 2b. Figures 2c and 2d illustrate the μ_1^e and μ_2^e parameters calculated throughout the model.

Table 3 – Performance of the methods for application 2

Method	Δt ($10^{-3}s$)	CPU Time (s)
CD	2.317(1.10)	831 (3.37)
EG-α	1.983 (1.00)	851 (3.46)
NB	4.338 (2.07)	891 (3.62)
New	4.155 (1.99)	673 (2.73)
New/sub	33.146[b] (15.96)	246 (1.00)

Table 3 shows the performance of the selected time-integration techniques for the given model. Once again, the new methodology outperforms the selected standard procedures in terms of CPU time, describing a more efficient approach. Displacement results (displacement modulus), computed using the explicit generalized α method and the new technique with multi-time-steps/sub-cycling splitting procedures, are presented in Figs.3 and 4, respectively. These figures reveal that the new methodology provides results similar to those of the EG-α, with the added benefit of fewer spurious oscillations in its computed responses. The logarithmic scale, which is adopted in these figures, aids in visualizing the referred displacement results.

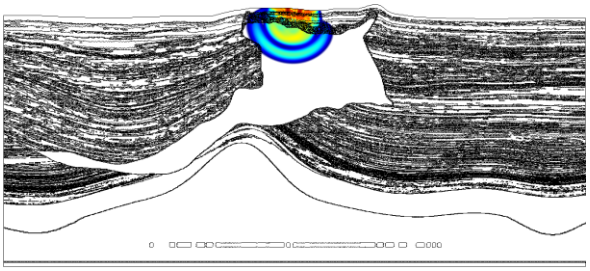

(a)

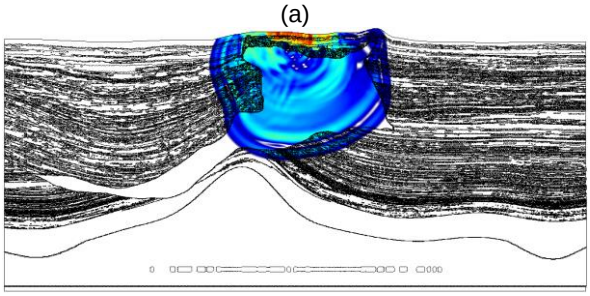

(b)

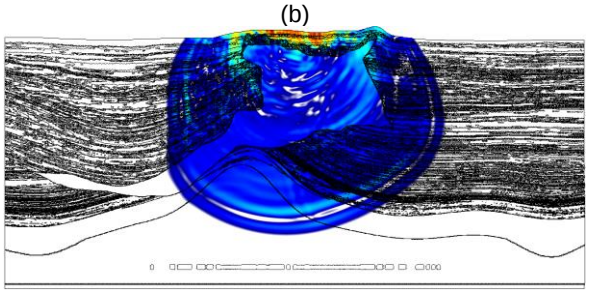

(c)

Fig.3 – Computed results for the EG-α, at different time instants: (a) 1s; (b) 2s; (c) 3s.

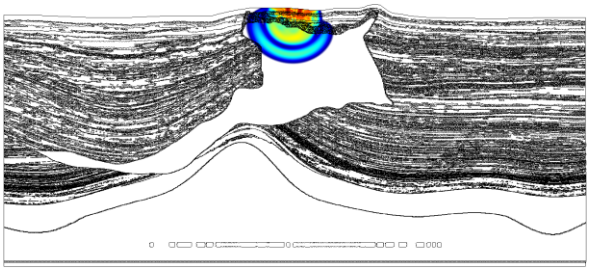

(a)

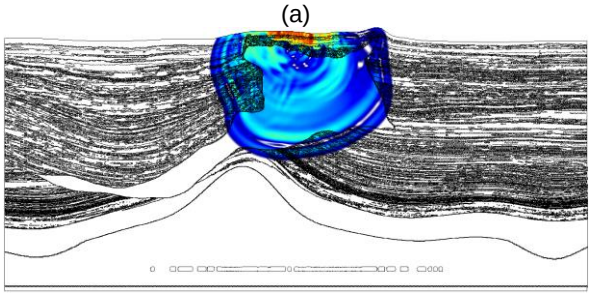

(b)

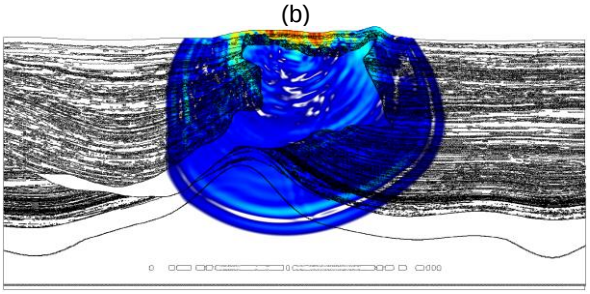

(c)

Fig.4 – Computed results for the new/sub, at different time instants: (a) 1s; (b) 2s; (c) 3s.

Conclusions

An explicit time-marching technique that incorporates subdomain/sub-cycling splitting procedures is discussed in this study for solving elastodynamic models. The time-steps and time-integration parameters of the method are locally and automatically determined based on the spatially discretized model's characteristics. The features of the discussed formulation may be summarized as follows: (i) it is a truly-explicit approach that does not require dealing with a system of equations, as lumped mass matrices are utilized; (ii) it is based on simple single-step displacement-velocity relations, making it a truly self-starting formulation; (iii) it allows for advanced controllable algorithmic dissipation by considering optimized, adaptive, locally computed parameters; (iv) it establishes a connection between the adopted temporal and spatial discretization methods, enabling better balancing of their errors; (v) it provides extended stability limits that may not be reduced by the introduction of physical damping, as in typical truly-explicit analyses; (vi) it is entirely automated and simple to apply, requiring no user effort or expertise; (vii) it is highly accurate and efficient, providing more effective analyses when combined with the developed subdomain/sub-cycling splitting procedures.

As it is illustrated in this paper, the discussed technique is highly versatile and produces effective results, consistently outperforming traditional time-marching methods. The

analyzed models demonstrate the robustness of the technique adapting to the properties of the model, as well as its ability to easily handle complex and highly refined large-scale problems, significantly reducing the computational burden of their solution process. As described, the discussed methodology stands as an effective time-marching technique, making it an attractive option for modeling complex wave propagation problems.

Acknowledgments

The financial support by CNPq (Conselho Nacional de Desenvolvimento Cientifico e Tecnológico), FAPEMIG (Fundação de Amparo à Pesquisa do Estado de Minas Gerais), PRH-ANP (Programa de Recursos Humanos da Agencia Nacional do Petróleo, Gás Natural e Biocombustíveis) and PETROBRAS (CENPES – 21066) is greatly acknowledged.

References

[1] Soares, D., Pinto, L. R., Mansur, W. J. (2023). A truly-explicit time-marching formulation for elastodynamic analyses considering locally-adaptive time-integration parameters and time-step values. *International Journal of Solids and Structures*, 112260.

[2] Noh, G., & Bathe, K. J. (2013). An explicit time integration scheme for the analysis of wave propagations. *Computers & structures*, 129, 178-193.

[3] Zhang, H.M., Xing, Y.F., (2019). Two novel explicit time integration methods based on displacement-velocity relations for structural dynamics. *Computers & structures*. 221, 127–141.

[4] Kim, W. (2019). An accurate two-stage explicit time integration scheme for structural dynamics and various dynamic problems. *International Journal for Numerical Methods in Engineering*, 120(1), 1-28.

[5] Loureiro, F. S., Silva, J. E. A., & Mansur, W. J. (2015). An explicit time-stepping technique for elastic waves under concepts of Green's functions computed locally by the FEM. *Engineering Analysis with Boundary Elements*, 50, 381-394.

[6] Soares, D. (2016). A novel family of explicit time marching techniques for structural dynamics and wave propagation models. *Computer Methods in Applied Mechanics and Engineering*, 311, 838-855.

[7] Soares, D. (2019). An adaptive semi-explicit/explicit time marching technique for nonlinear dynamics. *Computer Methods in Applied Mechanics and Engineering*, 354, 637-662.

[8] Soares, D. (2021). A multi-level explicit time-marching procedure for structural dynamics and wave propagation models. *Computer Methods in Applied Mechanics and Engineering*, 375, 113647.

[9] Soares, D. (2022). An enhanced explicit-implicit time-marching formulation based on fully-adaptive time-integration parameters. *Computer Methods in Applied Mechanics and Engineering*, in press.

[10] Soares Jr, D. (2022). An improved adaptive formulation for explicit analyses of wave propagation models considering locally-defined self-adjustable time-integration parameters. *Computer Methods in Applied Mechanics and Engineering*, 399, 115324.

[11] Soares, D. (2022). Three novel truly-explicit time-marching procedures considering adaptive dissipation control. *Engineering with Computers*, 38, 3251–3268.

[12] Belytschko, T., Smolinski, P., & Liu, W. K. (1985). Stability of multi-time step partitioned integrators for first-order finite element systems. *Computer Methods in Applied Mechanics and Engineering*, 49(3), 281-297.

[13] Pinto, L. R., Soares, D., & Mansur, W. J. (2021). Elastodynamic wave propagation modelling in geological structures considering fully-adaptive explicit time-marching procedures. *Soil Dynamics and Earthquake Engineering*, 150, 106962.

[14] Hulbert, G. M., & Chung, J. (1996). Explicit time integration algorithms for structural dynamics with optimal numerical dissipation. *Computer Methods in Applied Mechanics and Engineering*, 137(2), 175-188.

[15] Fehler, M. (2012). Seam update: Seam phase i rpsea update: Status of simulations. *The Leading Edge*, 31(12), 1424-1426